ISSN 2004-2965 Energy Proceedings, Vol. 24, 2021

International Conference on Applied Energy 2021
Nov. 29 - Dec. 5, 2021, Thailand/Virtual
Paper ID: 0183

Thermo-economic analysis and multi-objective optimization of a novel CCHP system driven by geothermal energy

Junrong Tang [1], Yi Que [2,*]

1. Key laboratory of low-grade Energy Utilization Technologies and Systems, Ministry of Education, School of Energy and Power Engineering, Chongqing University, Chongqing 400044, PR china
2. China Petroleum Engineering and Construction Corporation Southwest Company,Chengdu, Sichuan 610041, China

([*]Corresponding Author: sw@cnpc.com.cn)

ABSTRACT

Both effective utilization of renewable energy and multi-generation system are promising ways to reduce greenhouse gas emissions. This paper proposed a combined cooling, heating and power (CCHP) system, which is based on a basic system and consists of a transcritical CO_2 cycle, an ejector refrigeration cycle, a domestic water heater and a thermoelectric generator. The parametric and comparative analyses are performed to show the system performance enhancement of the modification system. The multi-objective optimization is also conducted for the involved CCHP systems. Results show that compared to basic system, the novel system owns a higher exergy efficiency (30.75 VS 27.42%) and a lower total product unit cost (27.39 VS 32.28 \$/GJ), confirming the obvious performance improvement.

Keywords: CCHP system; Transcritical CO_2 cycle; Ejector refrigeration cycle; Thermoelectric generator; Multi-objective optimization.

1. INTRODUCTION

The Chinese government has announced that china would hit peak emissions before 2030 and for carbon neutrality by 2060 on the 75th session of the UN General Assembly. To achieve this goal, on the one hand, it is of great use to employ renewable energy instead of fossil fuels for reducing greenhouse gas emissions. On the other hand, it is also important to develop multi-generation systems for improving energy conversion efficiency [1].

Unlike the strong intermittent nature of solar and wind energy, geothermal energy draws much attention because of the advantage of sustainability and reliability [2]. Many researchers have explored the utilization of geothermal energy to address the requirements of multiple kinds of energy. Zare [3] proposed two geothermal-driven combined cooling, heating and heating (CCHP) systems. This study used the organic Rankine cycle (ORC) and Kalina cycle (KC) for power generation for the two systems. Then, Wang et al. [4] employed a flash power cycle and absorption refrigeration (ARC) to supply the power and cooling energy. And the waste heat of ARC was recovered to produce heat water.

Although the above systems achieve the design purpose better, there are still two main problems: the complicated refrigeration cycle and the relatively low-efficiency power cycle. Thus, the ejector refrigeration cycle (ERC) was used instead of ARC due to the advantages of simple operation and low maintenance costs [5]. Meanwhile, the transcritical CO_2 (tCO_2) cycle was selected as the power unit for its better temperature match with the heat resource. As a natural working fluid, CO_2 has the advantages of zero ozone depression potential (ODP) and low Global Warming Potential (GWP). Moreover, the control and maintenance of the system can be easier because only CO_2 is used in the system. Therefore, it is a promising method to develop the CCHP system based on the tCO_2 cycle and ERC cycle. In this regard, Wang et al. [6] investigated a new CCHP system that combined a CO_2 Brayton cycle and an ERC. Then, Xu et al. [7] modified the CCHP system proposed by Wang et al. via adding an extraction turbine to improve the system efficiency. However, because of the large compressor power consumption, the above two systems may not provide extra power output. To solve this problem, V. Zare et al. [8] replaced the Brayton cycle with the Rankine cycle. They found that the new system can produce considerable net power output to realize the purpose of tri-generation better.

Selection and peer-review under responsibility of the scientific committee of the 13_{th} Int. Conf. on Applied Energy (ICAE2021).

Although the combined tCO_2-ERC based system has been studied widely, such systems still need several theoretical enhancements studies. And a comprehensive economic investigation also should be performed to evaluate the system performance. On basis of the conventional CCHP system [8], the gas cooler is replaced by an Internal Heat Exchanger (IHE) and a Thermoelectric Generator (TEG) is employed to recover some waste heat to power. TEG unit has been used widely in conventional power systems to improve system performance [9-11]. As a result, this paper proposed a novel enhanced geothermal enhanced ejector-based CO_2 (EEB-TEG) CCHP system for better system performance. A comprehensive parametric thermodynamic and economic analysis is performed for the basic and EEB-TEG CCHP systems. The optimal points for each system obtained with the best thermodynamic and economic performances are found.

2. SYSTEMS DESCRIPTION AND ASSUMPTIONS

2.1 Systems description

Fig.1 shows the EEB-TEG CCHP system. CO_2 absorbs thermal from hot geothermal water then reaches the supercritical state of high temperature (state 1). Supercritical CO_2 enters the turbine, expands to a lower pressure to drive a generator to generate electricity (State 2). The exhaust CO_2 releases heat through the heater to heat required domestic hot water (state 3), then enters the Internal Heat Exchanger (IHE) to preheat the working fluid before the gas heater. To drive the injector, stream 4 enters the ejector as the primary flow, after that it is mixed and diffused with the secondary flow from the evaporator (state 12). The CO_2 stream 5 from the ejector enters the hot side of TEG and the cooling water enters the cold side so that TEG generates some power from the waste heat. After that, the saturated liquid stream 6 is separated into two streams, one goes through the expansion valve (state 11) and enters the evaporator for cooling. While another stream is pumped to state 8 and flows through the IHX and gas heater in turn to complete the cycle. Fig.2 shows the basic system proposed by V. Zare et al. [8]. The main operation of this system is like the proposed system.

To simplify the model of the system and calculation, the following assumptions are made [5, 8, 12]:

(1) The system is in a steady state.

(2) The pressure drop of each heat exchanger and pipeline is ignored and there is no heat exchange between the system and environment.

(3) Assuming the outlet streams of condenser and evaporator are saturated.

(4) The geothermal fluid is considered to the pure water properties and the minimum temperature of that should be not less than 70°C.

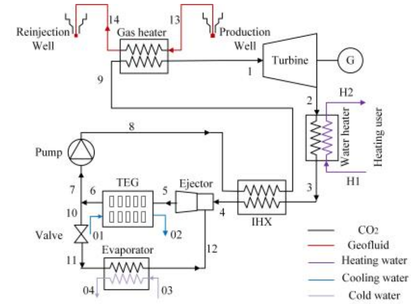

Fig. 1. Schematic diagrams of the EEB-TEG CCHP system.

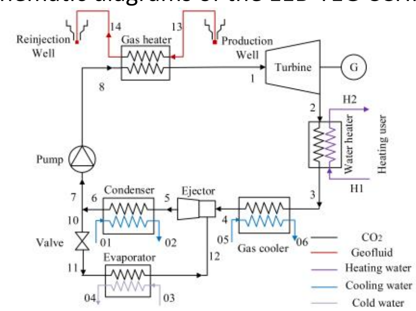

Fig. 2. Schematic diagrams of the basic CCHP system [8].

3. SYSTEM MODELING

3.1 Thermodynamic and Economic modeling

3.1.1 Thermodynamic modeling

According to the previous assumptions, mass and energy balance are applied to build the thermodynamic model of each component. And the exergy analysis also plays an important role in performance evaluation. Therefore, Table 1 summarizes the energy and exergy destruction relations for different components of the proposed system.

Table 1 Energy relations for the proposed system.

Component	Energy relations
Turbine	$\dot{W}_T = \dot{m}_1(h_1 - h_2)$
DWH	$\dot{Q}_{heat} = \dot{m}_2(h_2 - h_3) = \dot{m}_{hw}(h_{H2} - h_{H1})$
Ejector	$\dot{m}_4 h_4 + \dot{m}_{12} h_{12} = \dot{m}_5 h_5$
Pump	$\dot{W}_P = \dot{m}_7(h_8 - h_7)$
valve	$h_{11} = h_{10}$
Evaporator	$\dot{Q}_{eva} = \dot{m}_{11}(h_{12} - h_{11}) = \dot{m}_{03}(h_{03} - h_{04})$
Gas heater	$\dot{Q}_{in} = \dot{m}_1(h_1 - h_9) = \dot{m}_{13}(h_{13} - h_{14})$
IHX	$\dot{m}_3(h_3 - h_4) = \dot{m}_8(h_9 - h_8)$
TEG	$\dot{m}_5(h_5 - h_6) = \dot{m}_{01}(h_{02} - h_{01}) + \dot{W}_{TEG}$

This work chose the constant-pressure mixing model for ejector modeling [7]. And the losses of fluid in the ejector is considered by using the nozzle efficiency

(η_n), the mixing efficiency (η_m) and the diffuser efficiency (η_d). The flowchart for calculating the efficiencies and entrainment ratio (μ) of the ejector is given in Fig.2.

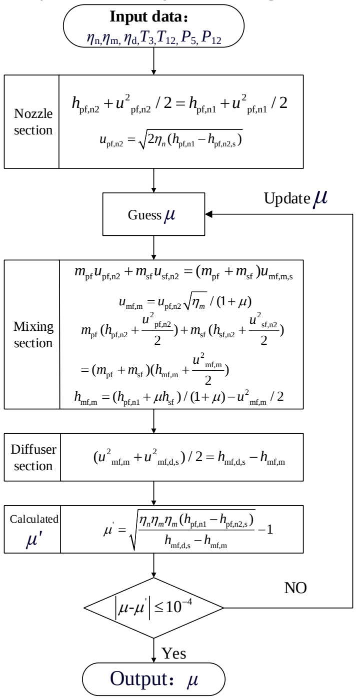

Fig.2 Flowchart of the ejector modeling.

For the TEG modeling, its efficiency can be expressed as follows [9, 12, 13]:

$$\begin{cases} \eta_{\mathrm{TEG}} = \eta_{Carnot}\dfrac{\sqrt{1+ZT_M}-1}{\sqrt{1+ZT_M}+\dfrac{T_L}{T_H}} \\ \eta_{\mathrm{TEG}} = \dfrac{\dot{W}_{\mathrm{TEG}}}{\dot{Q}_{ELEGANT}} \\ \dot{Q}_{ELEGANT} = \dot{m}_5(h_5 - h_6) \\ \eta_{Carnot} = 1 - \dfrac{T_L}{T_H} \end{cases}$$

where η_{carnot} is the equivalent Carnot cycle efficiency. T_H and T_L are the hot and cold sides temperatures of TEG. ZT_M is a key parameter that is multiplied by figure of merit (Z) and mean temperature.

3.1.2 Economic modeling

Economic analysis is an important tool to assess a novel thermal system. In this paper, the total cost rate for overall system are determined as follows[5, 14]:

$$\dot{C}_{tot} = \dot{C}_{\mathrm{fuel}} + \sum_i \dot{Z}_k \tag{1}$$

$$\dot{Z}_k = \left(\frac{CRF + \gamma_{\mathrm{k}}}{\mathrm{t}}\right) \bullet Z_k \tag{2}$$

where $\dot{C}_{\mathrm{fuel}}$ is the fuel cost rate. $\dot{Z}_k$ is the cost of the k_{th} component. The details of the above parameters and the cost functions of each component are provided in Table 2. All economic data should be compared in the same year via this equation [15].

$$original\ cost = reference\ cost \cdot \frac{cost\ index\ of\ the\ original\ year}{cost\ index\ of\ the\ reference\ year} \tag{3}$$

Table 2 Economic data for economic modeling [14, 16, 17].

Factor	Economic data
Useful operation years (n)	20
Interest rate (i_r)	12%
Maintenance factor (γ_K)	0.06
Annual plant operation hours (h)	7000
Capital recovery factor (CRF)	$CRF = \frac{i_r(1+i_r)^n}{(1+i_r)^n - 1}$
Components	Capital cost of equipment
Heat exchanger	$130 \cdot \left(\frac{A_K}{0.093}\right)^{0.78}$
Pump	$3540 \cdot W_p^{0.71}$
Turbine	$4405 \cdot W_{\mathrm{T}}^{0.7}$
Ejector	$1000 \cdot 16.14 \cdot 0.989 m \cdot (T_i / P_i^{0.05}) P_e^{-0.75}$
Expand valve	$114.5 \cdot m$
TEG	$1000 \cdot \dot{W}_{\mathrm{TEG}}$

3.2 Performance metrics

Based on the above models, energy and exergy efficiencies are used as indicators to evaluate the thermodynamic performance of the involved CCHP systems, as defined below:

$$\eta_{\mathrm{en}} = \frac{W_{net} + Q_{eva} + Q_{heat}}{Q_{\mathrm{in}}} \tag{4}$$

$$\eta_{ex} = \frac{W_{net} + E_{\mathrm{c}} + E_h}{E_{in}} \tag{5}$$

Where, W_{net} denotes the net power output of system, can be calculated from:

$$W_{net} = W_{\mathrm{T}} - W_{\mathrm{P}} + W_{\mathrm{TEG}} \tag{6}$$

Also, the total product unit cost ($c_{p,tot}$) is used as an indicator to evaluate the thermo-economic performance of proposed CCHP systems, as defined below [17]:

$$c_{p,tot} = \dot{C}_{tot} / (W_{net} + E_{\mathrm{c}} + E_h) \tag{8}$$

4. RESULTS AND DISCUSSIONS

4.1 Base condition analysis

In this section, the mathematical model is solved to explore the system performance enhancement of the proposed system using the input parameters presented in Table 3.

Table 3 Input data and basic assumption [5, 7, 8].

Parameter	Value
Environmental pressure (MPa)	0.101
Environmental temperature (°C)	15

Turbine inlet pressure (MPa)	15
Turbine outlet pressure (MPa)	7.8
Turbine isentropic efficiency (%)	85
Heater outlet temperature (°C)	50/T_3-10
Evaporator temperature (°C)	5
Geo- brine temperature (°C)	150
Geo-brine pressure (MPa)	0.5
Geo-brine mass flow rate (kg/s)	10
Pump isentropic efficiency (%)	70
Nozzle isentropic efficiency (%)	90
Mixing isentropic efficiency (%)	88
Diffuser isentropic efficiency (%)	85
Pinch point temperature difference (°C)	20
Ejector back pressure (MPa)	5.8

The performance metrics of involved systems under the base condition are shown in Fig.3. As can be seen, the EEB-TEG system has a better performance than the basic system. In detail, the energy and exergy efficiencies of the EEB-TEG system are 32.38% and 29.22%, which is 4.28% and 8.90% higher than that of the basic system, respectively.

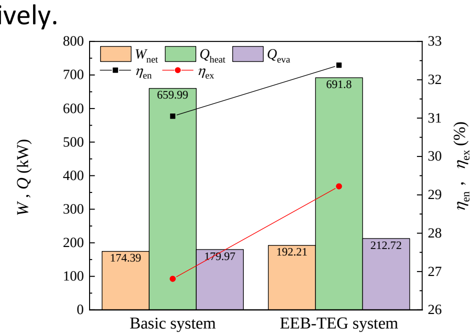

Fig 3. The performance metrics of involved systems under base condition.

4.2 Parametric analysis

Fig.4 shows the effects of turbine inlet pressure (P_1) on the performance of the three configurations. From Fig.4 (a), when P_1 increases, η_{ex} increases first and then decreases, while the opposite trend appears to be in the $c_{p,tot}$. It is mainly contributed to the higher turbine inlet pressure brings higher net power output of all systems, as shown in Fig.4 (b). It is also revealed that the Q_{heat} of involved systems decreases due to the decreasing turbine exhaust temperature caused by the increasing P_1. In addition, the higher P_1 increases the cooling capacity of systems, which is because the mass flow rate of the secondary flow into injector increases, resulting in an increasing working fluid entering the evaporator. To sum up, the variation of E_c and E_h for the cycle is the same as that of Q_{eva} and Q_{heat}. So η_{ex} increases in the case where the increase of W_{net} and E_c are dominant. Then η_{ex} decreases when the decrease of E_h becomes dominant. There is also similar relationship between the total investment cost and total useful energy, which can explain the trend of $c_{p,tot}$.

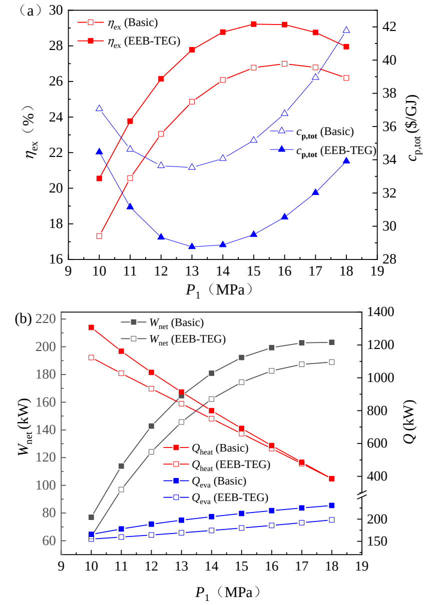

Fig. 4. Effects of P_1 on the system performance.

The effect of turbine outlet pressure (P_2) on the performance are presented in Fig.5. It can be seen that an increasing P_2 makes η_{ex} decreased, while $c_{p,tot}$ increases as P_2 changes. All these variations are the result of the combined effects of W_{net}, Q_{eva} and Q_{heat}. Referring to Fig.5(b), contrary to the effect of P_1, a large P_2 leads to the decrease of W_{net}. In addition, as P_2 increases under the condition of unchanged T_1, the gas heater inlet temperature also increases, then leading higher mass flow rate of CO_2. This also explains why Q_{heat} increases with P_2. The pump power consumption also increases with the increase of the working fluid flow, thus, the value of W_{net} falls. Fig.5 (b) also indicates that the cooling capacity is improved by increasing P_2. This is because the primary flow velocity away from the injector nozzle is increased by the change of P_2, leading to an increasing ejection rate of the injector. However, since W_{net} has greater influences than Q_{eva} and Q_{heat}, η_{ex} goes down with the increasing P_2. Similarly, the considerable increase in investment costs leads $c_{p,tot}$ to grow.

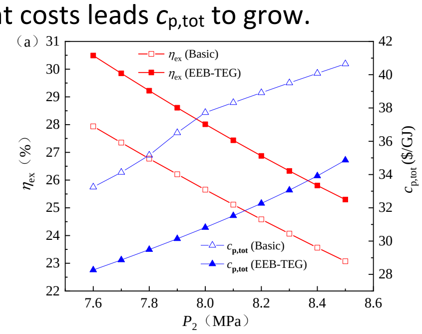

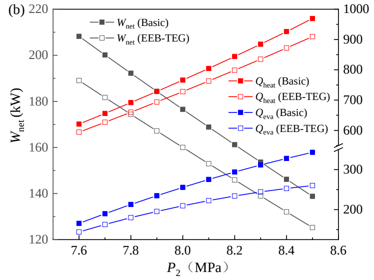

Fig. 5. Effects of P_2 on the system performance.

Fig.6 shows the variation of the performance of the involved systems with the evaporator temperature (Te). It can be seen from Fig.6 that the change of η_{ex} and $c_{p,tot}$ is very small when Te increases 0°C to 8°C. Fig.6 (b) shows that an increasing Te only causes the rise of the net power of EEB-TEG system. This is because the change of Te does not affect the basic system state point except for the flows in ERC. The same reason applies to explain why Q_{heat} keeps unchanged. Another thing that can be seen from Fig.6 (b) is that the increase in Te results in an improvement of cooling output (Q_{eva}). Consequently, the higher Q_{eva} brings out the growing trends of efficiencies. What's more, the higher Q_{eva} means the increase in investment of evaporator, thus $c_{p,tot}$ grows up.

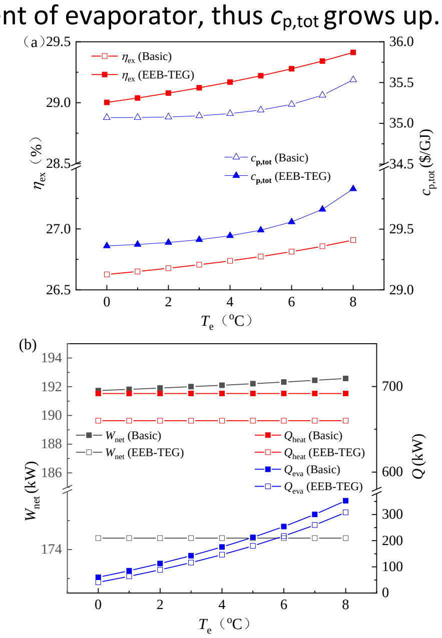

Fig. 6. Effects of T_e on the system performance.

The effect of ZT_M on the performance of the EEB-TEG system is shown in Fig.7. When ZT_M rises, better system performance is obtained as expected. It can be explained by the rising W_{net} caused by TEG unit at higher ZT_M. Moreover, although the total cost investment of the system increases with the increasing ZT_M, the enhancement of W_{net} has dominated the trend of $c_{p,tot}$, thus $c_{p,tot}$ decreases.

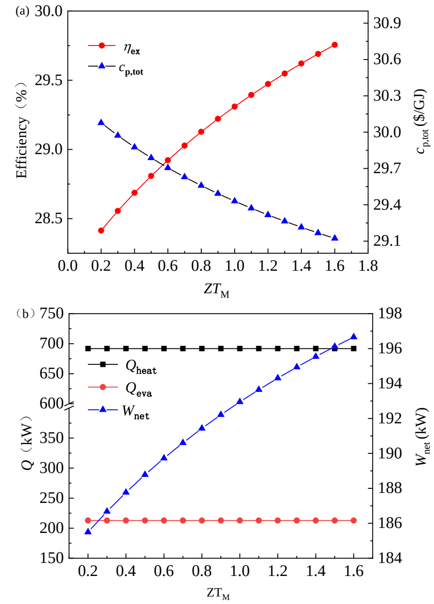

Fig. 7. Effects of ZT_M on the system performance.

4.3 Multi-objective optimization

This section conducts multi-objective optimization (MOO) to balance the thermodynamic and economic performance of the involved system. The NSGA-II is selected as the optimization algorithm . The boundaries of decision variables are outlined in Table 4 [8, 17].

Table 4 Boundaries of decision variables for MOO.

Items	System a	System c
P_1 (MPa)	10-18	10-18
P_2 (MPa)	7.6-8.5	7.6-8.5
T_e (°C)	0-8	0-8
ZT_M	/	0.2-1.6

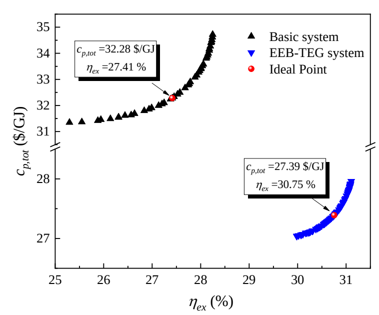

Fig. 8. Optimal Pareto frontiers for involved CCHP systems.

In this paper, η_{ex} (to be maximized) and $c_{p,tot}$ (to be minimized) are selected as the objective functions. Fig.8 shows the Pareto frontiers for involved systems. And the final optimal solution is marked as a red ball. Referring to Fig.8, the optimal η_{ex} of EEB-TEG system (30.75%) is higher than that of basic system (27.42%) by 12.14%. In additition, $c_{p,tot}$ of the EEB-TEG system is decreased by 15.14%. Both thermodynamic and economic performances are obtained from EEB-TEG system.

5. CONCLUSION

This paper proposed a novel enhanced geothermal enhanced ejector-based CO_2 (EEB-TEG) CCHP system to afford different energy demands. The thermo-economic, parametric analysis and multi-objective optimization analysis are performed for the basic and EEB-TEG CCHP systems. Compared to the basic system, the EEB-TEG CCHP system can own an improvement of η_{ex} by 12.14% and $c_{p,tot}$ by 15.14%, respectively.

ACKNOWLEDGEMENT

This work is supported by the National Natural Science Foundation of China (No.51876015).

REFERENCE

[1] Pan M, Lu F, Zhu Y, Li H, Yin J, Liao Y, et al. 4E analysis and multiple objective optimizations of a cascade waste heat recovery system for waste-to-energy plant. Energy Conversion and Management. 2021;230.

[2] Alibaba M, Pourdarbani R, Manesh MHK, Ochoa GV, Forero JD. Thermodynamic, exergo-economic and exergo-environmental analysis of hybrid geothermal-solar power plant based on ORC cycle using emergy concept. Heliyon. 2020;6:e03758.

[3] Zare V. A comparative thermodynamic analysis of two tri-generation systems utilizing low-grade geothermal energy. Energy Conversion and Management. 2016;118:264-74.

[4] Wang J, Ren C, Gao Y, Chen H, Dong J. Performance investigation of a new geothermal combined cooling, heating and power system. Energy Conversion and Management. 2020;208.

[5] Mosaffa AH, Farshi LG. Thermodynamic and economic assessments of a novel CCHP cycle utilizing low-temperature heat sources for domestic applications. Renewable Energy. 2018;120:134-50.

[6] Wang J, Zhao P, Niu X, Dai Y. Parametric analysis of a new combined cooling, heating and power system with transcritical CO2 driven by solar energy. Applied Energy. 2012;94:58-64.

[7] Xu XX, Liu C, Fu X, Gao H, Li Y. Energy and exergy analyses of a modified combined cooling, heating, and power system using supercritical CO2. Energy. 2015;86:414-22.

[8] Zare V, Rostamnejad Takleh H. Novel geothermal driven CCHP systems integrating ejector transcritical CO2 and Rankine cycles: Thermodynamic modeling and parametric study. Energy Conversion and Management. 2020;205.

[9] Gholamian E, Habibollahzade A, Zare V. Development and multi-objective optimization of geothermal-based organic Rankine cycle integrated with thermoelectric generator and proton exchange membrane electrolyzer for power and hydrogen production. Energy Conversion and Management. 2018;174:112-25.

[10] Zare V, Palideh V. Employing thermoelectric generator for power generation enhancement in a Kalina cycle driven by low-grade geothermal energy. Applied Thermal Engineering. 2018;130:418-28.

[11] khanmohammadi S, Saadat-Targhi M. Performance enhancement of an integrated system with solar flat plate collector for hydrogen production using waste heat recovery. Energy. 2019;171:1066-76.

[12] Rostamnejad Takleh H, Zare V. Employing thermoelectric generator and booster compressor for performance improvement of a geothermal driven combined power and ejector-refrigeration cycle. Energy Conversion and Management. 2019;186:120-30.

[13] Khanmohammadi S, Musharavati F, Kizilkan O, Duc Nguyen D. Proposal of a new parabolic solar collector assisted power-refrigeration system integrated with thermoelectric generator using 3E analyses: Energy, exergy, and exergo-economic. Energy Conversion and Management. 2020;220.

[14] Moghimi M, Emadi M, Ahmadi P, Moghadasi H. 4E analysis and multi-objective optimization of a CCHP cycle based on gas turbine and ejector refrigeration. Applied Thermal Engineering. 2018;141:516-30.

[15] Mignard D. Correlating the chemical engineering plant cost index with macroeconomic indicators. Chemical Engineering Research and Design. 2014;92:285-94.

[16] Dhahad HA, Hussen HM, Nguyen PT, Ghaebi H, Ashraf MA. Thermodynamic and thermoeconomic analysis of innovative integration of Kalina and absorption refrigeration cycles for simultaneously cooling and power generation. Energy Conversion and Management. 2020;203.

[17] Zhang Q, Luo Z, Zhao Y, Cao R. Performance assessment and multi-objective optimization of a novel transcritical CO2 trigeneration system for a low-grade heat resource. Energy Conversion and Management. 2020;204.